Control of a Two-Wheeled Inverted Pendulum using Integral Sliding Mode

Ravindra K. Munje

K. K. Wagh Institute of Engineering Education and Research, Nashik 422003, India, ravimunje@yahoo.co.in

Deepak M. Sonje

R. H. Sapat College of Engineering, Management Studies and Research, Nashik 422009, India, deepaksonje123@gmail.com

Deepak P. Kadam

MET's Institute of Engineering, Nashik 422003, India, dpkadam@gmail.com

Abstract -

Modelling and control of two-wheeled inverted pendulum (TWIP) are gaining much interest due to the advancements in hardware and computing technologies. TWIP system has many advantages and applications. However, it is still having many challenges to control when faced with tasks of positioning, disturbance rejection, parameter uncertainties, etc. In this paper, a control scheme based on modern control techniques is presented to overcome these issues. In this, a robust integral sliding mode controller (ISMC) is proposed for the nonlinear system of TWIP. First of all, a robust integral sliding mode controller is designed to tackle short-term and long-term constant and time-varying disturbances and issues related to parameter variations. Then, it is applied to the nonlinear model of TWIP and performance is observed under different transient conditions. A comparison with prevalent controllers in the literature is carried out. From this, a significant improvement is seen with the proposed controller for all types of transients. This paper also discusses the software Simulink realization of modelling and control of TWIP, which can be valuable for novices working in this area.

Index Terms - Integral Sliding Mode, Simulink Modeling, Sliding Mode Control, Two-Wheeled Inverted Pendulum.

INTRODUCTION

The two-wheeled inverted pendulum (TWIP) is a highly nonlinear and naturally unstable system. It is an underactuated system having three degree-of-freedom with pitch, yaw and straight-line movements merely with two wheels [1]. This interesting system has attracted the attention of many researchers worldwide over the last three decades. However, there are some challenges. Challenges associated with this system are mathematical modelling, controller design and its implementation. Although the modelling is difficult due to nonlinear and complex dynamics, uncertain environmental conditions, parameter uncertainties, etc. several research groups have proposed mathematical models for TWIP. An exact and accurate nonlinear model of the TWIP system is proposed in [2]. This model overcomes the drawbacks of the earlier models such as inappropriate assumptions, improper terms, missing some important terms, etc. Followed by modelling, control design plays an important role. In literature, the controllers for TWIP are designed using the linear quadratic regulator (LQR) [3], feedback linearization [4], fuzzy logic [5, 6], sliding mode control [7], optimal control [8], etc.

In [9], a gray box modelling of a TWIP robot using the Lagrange equation is proposed, in which a closed-loop parameter identification method is used. Further, in this, the design and software implementations of PID and LQR are demonstrated. In another research, the model of TWIP is obtained using differential equations, and then PID, LQR and linear quadratic Gaussian (LQG) controllers are designed. It is also shown that the performance of LQG is superior to LQR [10]. In [11], an optimal controller based on model predictive control is designed to show the performance improvement over PID for the self-balancing two-wheeled robot system. In [12], an integral sliding

mode controller (ISMC) is designed and the performance is compared with [11]. However, a disturbance is not considered in this case. Nevertheless, in all the above designs, the 4th order model is used to design the controller, i.e. yaw motion dynamics are not considered.

In [13], the Newton-Euler method is used to derive a mathematical model of the two-wheeled self-balancing robot. The LQR is designed for the linear system and the influence of Q and R on the system state is analyzed. Very recently, an underactuated sliding mode control scheme is implemented using a variety of control parameters [14]. The controller performance is successfully tested for set-point changes and disturbance conditions using MATLAB simulation. In [15], the controller is designed to keep the TWIP in an upright position and prevent it from tipping over when the TWIP is subjected to either unexpected impulses, or to shift weights along with its chassis. In [16], different controllers are tested for an inverted pendulum system. In this work, LQR, pole placement, and PID are designed for the simulation. Nonetheless, the control designs discussed so far are applied to the linearized models of the TWIP. In [17], PID is designed for a mobile robot using an optimization technique. However, limited simulation cases are discussed.

From the literature survey, it can be seen that the development of an accurate mathematical model and design of the control algorithm which can give asymptotic stabilization in the presence of a disturbance environment are tedious tasks for TWIP. Some controllers work well for steady disturbances and some for dynamic disturbances. Very few controllers are available for alleviating both the disturbance situations.

This paper aims at designing an integral sliding mode controller for a TWIP system achieving steady-state and transient performance. The transient performance of the said system is examined with all types of disturbances. The main contributions of the paper are as given below.

(1) Designing an integral sliding mode controller for achieving both acceptable steady-state and transient performance. Here, the transient performance is tested for the disturbances like constant (temporary and continuous) step, sinusoidal (time-varying) disturbances, and parameter variations,

(2) Demonstrating the applicability of the proposed control scheme on the 6th-order nonlinear model of TWIP with realizable Simulink blocks.

To show the effectiveness of the suggested controller the simulation results are compared with an existing controller.

The rest of the paper is organized as follows. In Section 2, the nonlinear mathematical model of the TWIP is discussed. In Section 3, the design of an integral sliding mode controller is presented. The simulation results and discussions are presented in Section 4. Finally, the paper is concluded in Section 5.

DYNAMIC MODEL OF TWIP SYSTEM

Recently a comprehensive mathematical model of TWIP has been proposed in [2, 8]. The same model is used here for exploring the possibility of an integral sliding mode controller. This model is given by the following nonlinear equations:

$$\dot{x}_1 = x_2 \tag{1}$$

$$\dot{x}_2 = a_2(x)x_3 + b_2(x)(T_L + T_R) \tag{2}$$

$$\dot{x}_3 = x_4 \tag{3}$$

$$\dot{x}_4 = a_4(x)x_3 + b_4(x)(T_L + T_R) \tag{4}$$

$$\dot{x}_5 = x_6 \tag{5}$$

$$\dot{x}_6 = a_6(x)x_3 + b_6(x)(T_L - T_R) \tag{6}$$

where x_1, x_3 and x_5 are respectively straight, pitch (θ) and yaw (ψ) motions and x_2, x_4 and x_6 are corresponding time derivatives. This system is of order six with two inputs T_L and T_R, i.e. torques applied to the left and right wheels respectively. The functions $a_i(x)$ and $b_i(x)$, in (1)-(6), are given by the following equations.

$$a_2(x) = \frac{1}{\eta_1(x_3)} \frac{sinx_3}{x_3} [p_5 \cos \cos x_3 + p_6 x_4^2 + p_7 x_6^2 + p_8 cos^2 x_3 x_6^2] \tag{7}$$

$$a_4(x) = \frac{1}{\eta_1(x_3)} \frac{sinx_3}{x_3} [p_9 + p_{10}x_4^2 cosx_3 + p_{11}cosx_3x_6^2] \qquad (8)$$

$$a_6(x) = \frac{1}{\eta_2(x_3)} \frac{sinx_3}{x_3} [p_{12}x_4x_6 cosx_3 + p_{13}x_2x_6] \qquad (9)$$

$$b_2(x) = \frac{1}{\eta_1(x_3)} [p_{14}cosx_3 + p_{15}] \qquad (10)$$

$$b_4(x) = \frac{1}{\eta_1(x_3)} [p_{16}cosx_3 + p_{17}] \qquad (11)$$

$$b_6(x) = \frac{1}{\eta_2(x_3)} [p_{18}] \qquad (12)$$

with

$$\eta_1(x_3) = [p_1 + p_2 sin^2 x_3] \qquad (13)$$

$$\eta_2(x_3) = [p_3 + p_4 sin^2 x_3] \qquad (14)$$

where p_i's and other parameters are given below

$$p_1 = m_B I_2 + 2(m_W + (J/r^2))(I_2 + m_B l^2) \qquad (15)$$

$$p_2 = (m_B l)^2 \qquad (16)$$

$$p_3 = I_3 + 2J_v + 2(m_W + (J/r^2))d^2 \qquad (17)$$

$$p_4 = I_1 + m_B l^2 - I_3 \qquad (18)$$

$$p_5 = -(m_B l)^2 g \qquad (19)$$

$$p_6 = (I_2 + m_B l^2) m_B l \qquad (20)$$

$$p_7 = m_B l I_2 + m_B^2 l^3 \qquad (21)$$

$$p_8 = m_B l(I_3 - I_1 - m_B l^2) \qquad (22)$$

$$p_9 = (m_B + 2m_W + 2(J/r^2))(m_B lg) \qquad (23)$$

$$p_{10} = -p_2 \qquad (24)$$

$$p_{11} = -((m_B l)^2 + (I_3 - I_1 - m_B l^2)(m_B + 2m_W + 2(J/r^2))) \quad (25)$$

$$p_{12} = 2(I_3 - I_1 - m_B l^2) \qquad (26)$$

$$p_{13} = -m_B l \qquad (27)$$

$$p_{14} = -p_{13} \qquad (28)$$

$$p_{15} = (I_2 + m_B l^2)/r \qquad (29)$$

$$p_{16} = -p_{13}/r \qquad (30)$$

$$p_{17} = m_B + 2m_W + 2(J/r^2) \qquad (31)$$

$$p_{18} = -d/r \qquad (32)$$

All p_i's are constants calculated from system parameters. The values of all parameters in p_i with their meaning are given in Table 1. The equations (1)-(6) are linearized using the Taylor series approximation. The steady-state values for states and inputs are taken as zero. It is then represented in the standard state-space form as

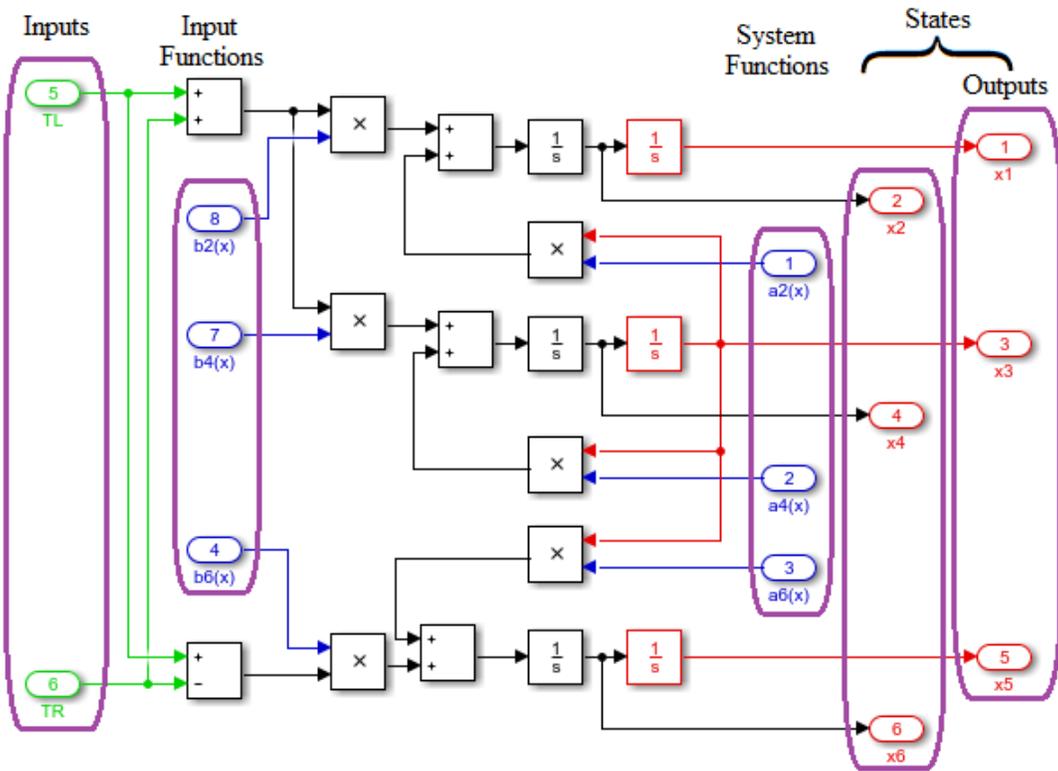$$\dot{x}(t) = Ax(t) + Bu(t) \qquad (33) \qquad y(t) = Cx(t) \qquad (34)$$

FIGURE. 1

NONLINEAR SIMULINK MODEL OF THE TWIP SYSTEM

with the state, input and output vectors as

$$x = [x_1 \ x_2 \ x_3 \ x_4 \ x_5 \ x_6 \ ]^T, \qquad\qquad (35)$$

$$u = [T_L \ T_R \ ]^T \qquad\qquad (36)$$

$$y = [x_1 \ x_3 \ x_5 \ ]^T. \qquad\qquad (37)$$

TABLE 1

PARAMETER VALUES FOR THE TWIP [8].

Symbols	Meaning of symbols	Values
d	Distance between wheels	0.6 m
m_B	Mass of pendulum body	45 kg
m_W	Mass of wheel	2 kg
l	Length of the pendulum rod	0.135 m
r	Radius of wheels	0.2032 m
I_1	Moment of Inertia of pendulum body for b_1	1.9 kg m^2
I_2	Moment of Inertia of pendulum body for b_2	2.1 kg m^2
I_3	Moment of Inertia of pendulum body for b_3	1.6 kg m^2
J	Moment of Inertia of a wheel for the wheel axis	0.02 kg m^2
J_v	Moment of Inertia of a wheel for the vertical axis	0.04 kg m^2
g	Acceleration due to gravity	9.81 m/s^2

The eigenvalues of (33) are found to be (-5.2267, 0, 0, 0, 0, 5.2267), i.e. the system is open-loop unstable. But the system is found to be controllable. Controllability plays an important role in controller design. Responses for the zero input conditions are zero for both linear and nonlinear models.

It must be noted that, although the controller is designed using a linear model, it is tested on the nonlinear system developed in MATLAB Simulink [19] as shown in Figure 1. In Figure 1, only the final subsystem (realization of (1)-(6)) is shown with clear indications for inputs (T_L and T_R), input functions ($b_i(x)$), system functions ($a_i(x)$), outputs (x_1, x_3, x_5), and states (x_1 to x_6). Other subsystems of input and system functions are not shown. These subsystems can be developed in the same way as that of Figure 1 using equations (7)-(14) and values in Table 1. In the following section, an integral sliding mode controller (ISMC) is designed.

ROBUST INTEGRAL SLIDING MODE CONTROLLER

Let us consider a linear system with parametric uncertainties, unmodeled dynamics and external disturbances, represented as

$$\dot{x}(t) = (A + \Delta A)x(t) + (B + \Delta B)u(t) + \xi(t), \qquad (38)$$
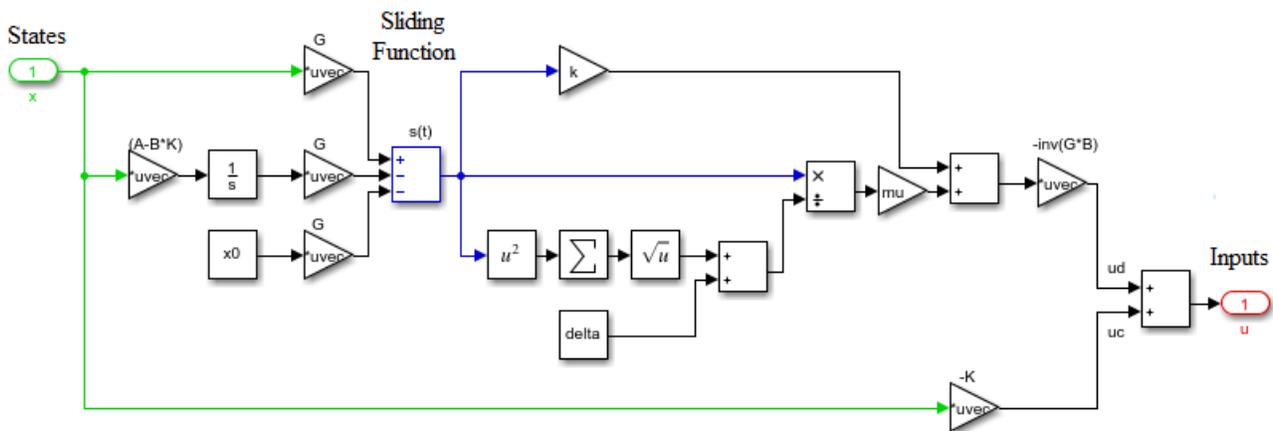
$$y(t) = Cx(t), \qquad (39)$$

FIGURE. 2
SIMULINK MODEL OF ISMC SIGNAL GENERATION

where $x \in R^n$ is the state, $u \in R^m$ is input and $y \in R^p$ is output. A, B and C are the known real constant matrices with appropriate dimensions. Furthermore, ΔA and ΔB are parametric uncertainties and $\xi(t)$ represents the uncertainty due to unmodeled dynamics and external disturbances affecting the system. The following assumptions are made.

Assumption 1: System (A, B) is controllable.

Assumption 2: Parametric uncertainties, unmodeled dynamics and external disturbances are unknown but bounded and satisfy the matching condition, i.e. $\xi(t) \in span(B)$.

From Assumption 2, let system uncertainties be written as

$$\Delta Ax(t) + \Delta Bu(t) + \xi(t) = BD\xi(t), \qquad (40)$$

where $\xi(t) \in R^l$ and $D \in R^{m \times l}$. With (40), the system (38) can be written as

$$\dot{x}(t) = Ax(t) + B(u(t) + D\xi(t)) \qquad (41)$$

The objective is to design a robust controller for the system (41), such that the system becomes insensitive to uncertainties and external disturbances. Let us assume that the control input $u(t)$ has two parts, i.e. a continuous part and a discontinuous part defined as

$$u(t) = u_c(t) + u_d(t) \qquad (42)$$

where $u_c(t)$ is the continuous control and $u_d(t)$ is the discontinuous control. With (42), the system (41) becomes

$$\dot{x}(t) = Ax(t) + B(u_c(t) + u_d(t) + D\xi(t)) \qquad (43)$$

In this, the continuous control $u_c(t)$ is designed using the eigenvalue assignment technique, and discontinuous control $u_d(t)$ is designed using the ISMC technique [19].

3.1 Design of Continuous Control

Continuous control $u_c(t)$ is designed for a nominal system. Hence, neglecting the uncertain part in (43) one can get a nominal system as

$$\dot{x}(t) = Ax(t) + Bu_c(t) \qquad (44)$$

In this, the control input is given by

$$u_c(t) = -Kx(t) \qquad (45)$$

where $K \in R^{m \times n}$ is a state-feedback gain matrix designed such that $\lambda_{desired} = \lambda(A - BK)$, where $\lambda(.)$ are eigenvalues of the system and $\lambda_{desired}$ are desired eigenvalues. It must be noted that the controller (45) may not be able to control the uncertain system (43) directly. To tackle the uncertainties present in the system, the controller is required to be combined with ISMC which guarantees robustness throughout the motion.

3.2 Design of Discontinuous Control

Let us define the sliding surface as

$$s(t) = Gx(t) + z(t) \qquad (46)$$

where $G \in R^{m \times n}$ provides freedom to the designer and $z(t) \in R^m$ induces the integral term. During sliding, $s(t) = \dot{s}(t) = 0$ and, therefore, from (46)

$$\dot{s}(t) = G\dot{x}(t) + \dot{z}(t) = 0 \qquad (47)$$

Substituting $\dot{x}(t)$ from (43) in (47) and compensating matched uncertainty, i.e., $(u_d(t))_{eq} = -D\xi(t)$ one can get

$$\dot{z}(t) = -G(Ax(t) + Bu_c(t)) \qquad (48)$$

Integrating (48) gives $z(t)$. Substituting this in (46) with initial condition $z(0) = -Gx(0)$ gives

$$s(t) = Gx(t) - Gx(0) - G\int_0^t (Ax(\tau) + Bu_c(\tau))d\tau \qquad (49)$$

where G is chosen as the left pseudo-inverse of B, making GB invertible and ensuring $-Gx(0)$ makes $s(0) = 0$, thereby eliminating the reaching phase. This particular choice of G reduces the amplitude of chattering [20]. The discontinuous control $u_d(t)$ is designed based on exponential reaching law [21-22] as

$$u_d(t) = -(GB)^{-1}(\mu\, sgn(s(t)) + ks(t)) \qquad (50)$$

where μ is constant with $\mu > 0$. From (42), (45), and (50), the control law $u(t)$ is given as

$$u(t) = -Kx(t) - (GB)^{-1}(\mu\, sgn(s(t) + ks(t)) \qquad (51)$$

Chattering is overcome by using a boundary layer technique where the $sgn(.)$ function is replaced by $\frac{s}{|s|+\delta}$. In this, δ is a small positive design scalar. Using (51), a practical control law is obtained as

$$u(t) = -Kx(t) - (GB)^{-1}\left(\mu \frac{s(t)}{|s(t)|+\delta} + ks(t)\right) \qquad (52)$$

The MATLAB implementation of (52) is illustrated in Figure 2. All the states of the system (shown in Figure 1) are the inputs to Figure 2 and the output is the control signal (52). This control signal is fed back to the inputs in Figure 1. In the next section, the simulation results and discussions are presented.

SIMULATION RESULTS AND DISCUSSIONS

Initially, the state feedback gain matrix is determined for the linear system of TWIP, as given in (45), to place eigenvalues at $(-6, -4.5, -3 \pm 0.5i, -1.5 \pm 0.25i)$. After that, the discontinuous control signal (50) is formulated with $\mu = 2$ and $k = 3$. Next, the total control input (52) is constructed using (45) and (50). Then the complete closed-loop system is simulated with the nonlinear model of TWIP. The initial conditions for the nonlinear model of TWIP are arbitrarily selected as $(0.1, 0, 0.2, 0, 0.3, 0)$ for checking the regulation performance.
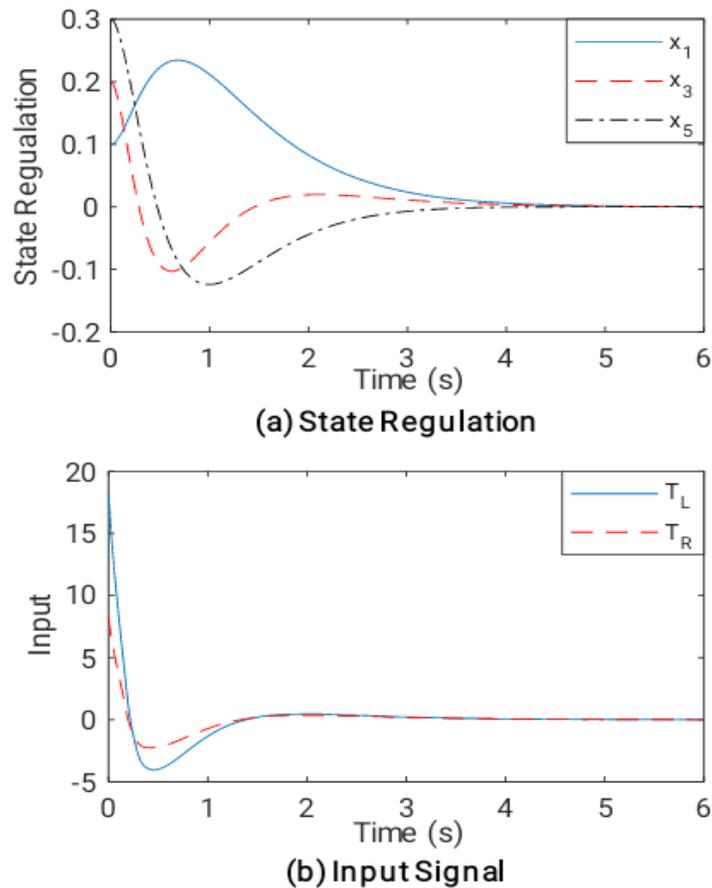

(a) State Regulation

(b) Input Signal

FIGURE 3

REGULATION RESPONSE OF THE SYSTEM

The regulation performance with ISMC is observed with the initial conditions mentioned above. It is illustrated in Figure 3. From Figure 3(a) it can be noticed that all the outputs are regulated and attain a steady state within 5 s. Figure 3(b) represents the responses of input signals. Although the regulation response is not plotted for all the states, it is found to be satisfactory.

The second simulation experiment is conducted with continuous disturbance applied to both wheels. The disturbance applied to the left wheel is $d_L = 0.3sin(t)$ and to the right wheel is $d_R = 0.3cos(t)$. With this, the responses are obtained as shown in Figure 4. In this, the performance is compared with the linear quadratic regulator, as they both have the same feedback gain matrix. From Figure 4 it can be seen that the response with the simple LQR is oscillatory with constant frequency and that with the proposed ISMC is steady.
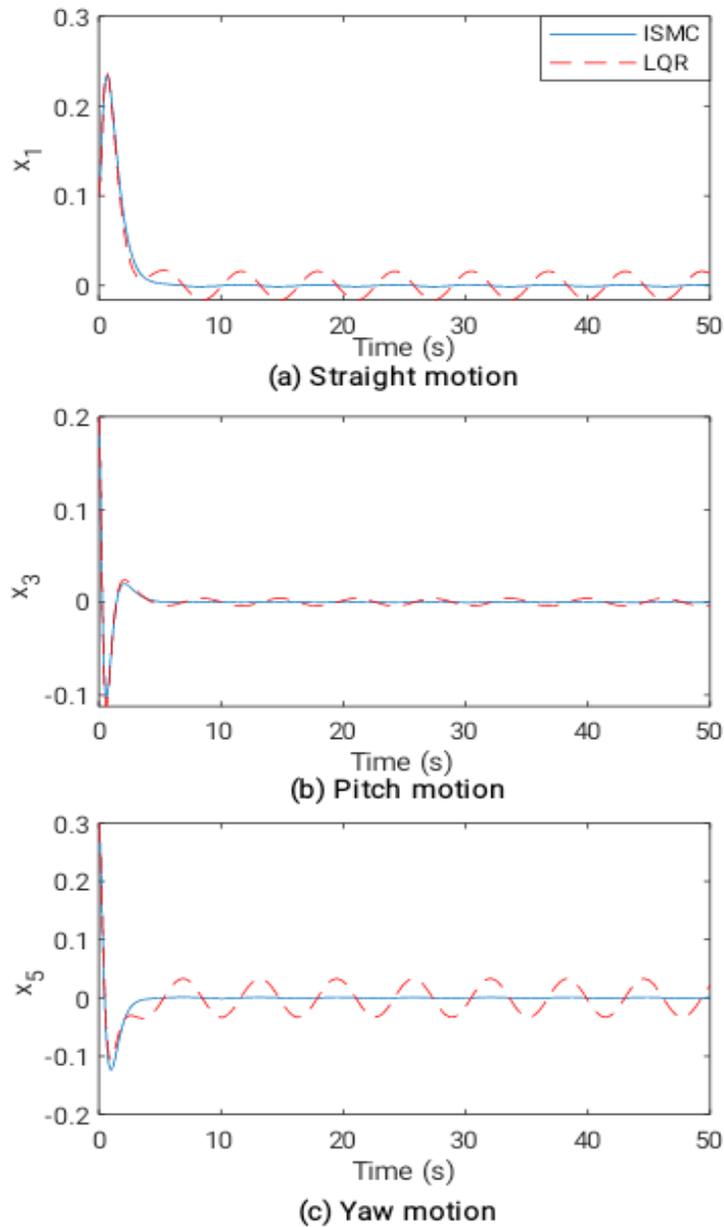

FIGURE 4

RESPONSE TO THE CONTINUOUS DISTURBANCE

In the third simulation, the constant disturbance, $d = 0.3\ N$, of short interval (20 s) is applied to the left wheel. The disturbance is applied at 10 s and removed at 30 s. The response is plotted in Figure 5 and is compared with LQR. Here also the performance of ISMC is found to be unaffected and in a system with LQR small variations at the start of disturbance and at the time of removal of disturbance can be noticed. In fact, with LQR for Straight and Yaw motions, there are some steady-state errors. This shows that the performance of the proposed ISMC is robust.
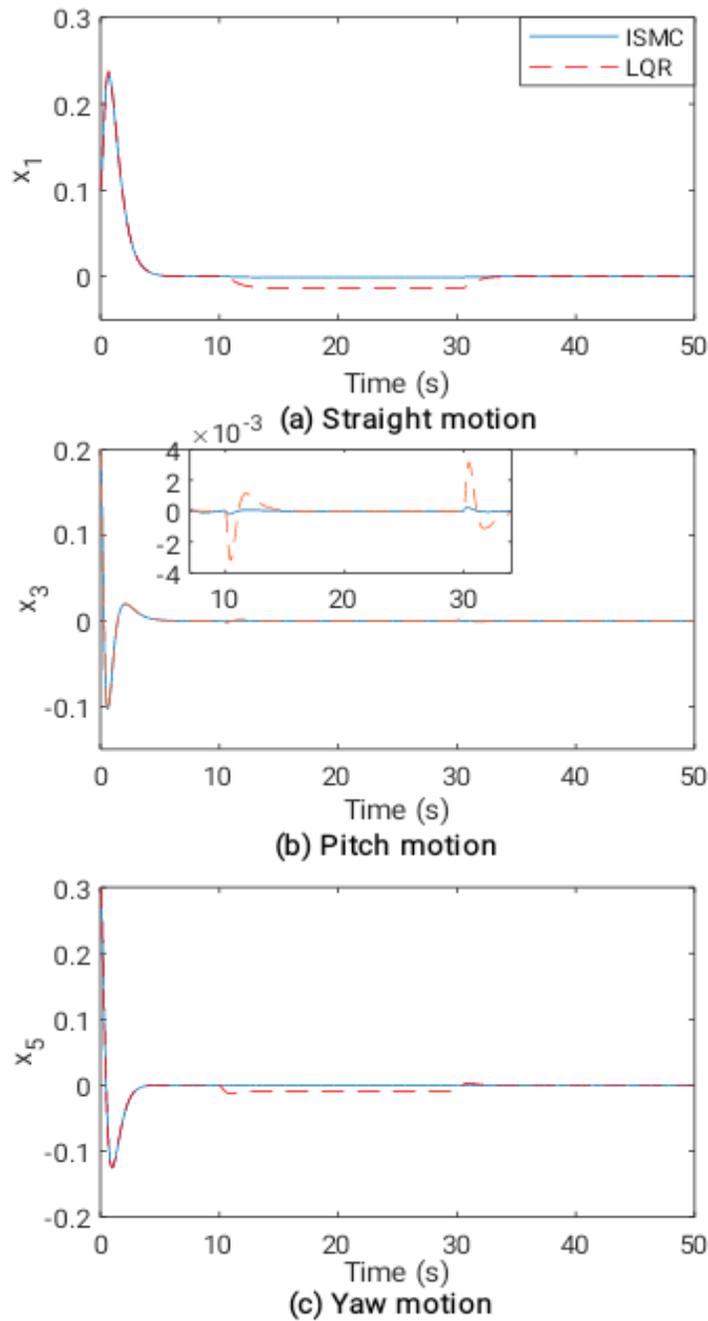
FIGURE 5

RESPONSE TO CONSTANT DISTURBANCE

In the last simulation, a case of parameter variations is considered. In this, all the parameters of the system, listed in Table 1, are changed slowly. It is observed that after a 45 % change in the parameters, the performance with the LQR becomes unstable. Hence, all the parameters are increased by 45% and responses are plotted as shown in Figure 6. It is noticed that the performance of the proposed ISMC is much better than the LQR.

Apart from the simulation waveform comparison, the comparison is also done for the error performance indices, namely integral time square error (ITSE) and integral time absolute error (ITAE), as shown in Table 2, calculated for outputs x_1, x_3 and x_5 shown in Figures 4, 5 and 6 respectively.
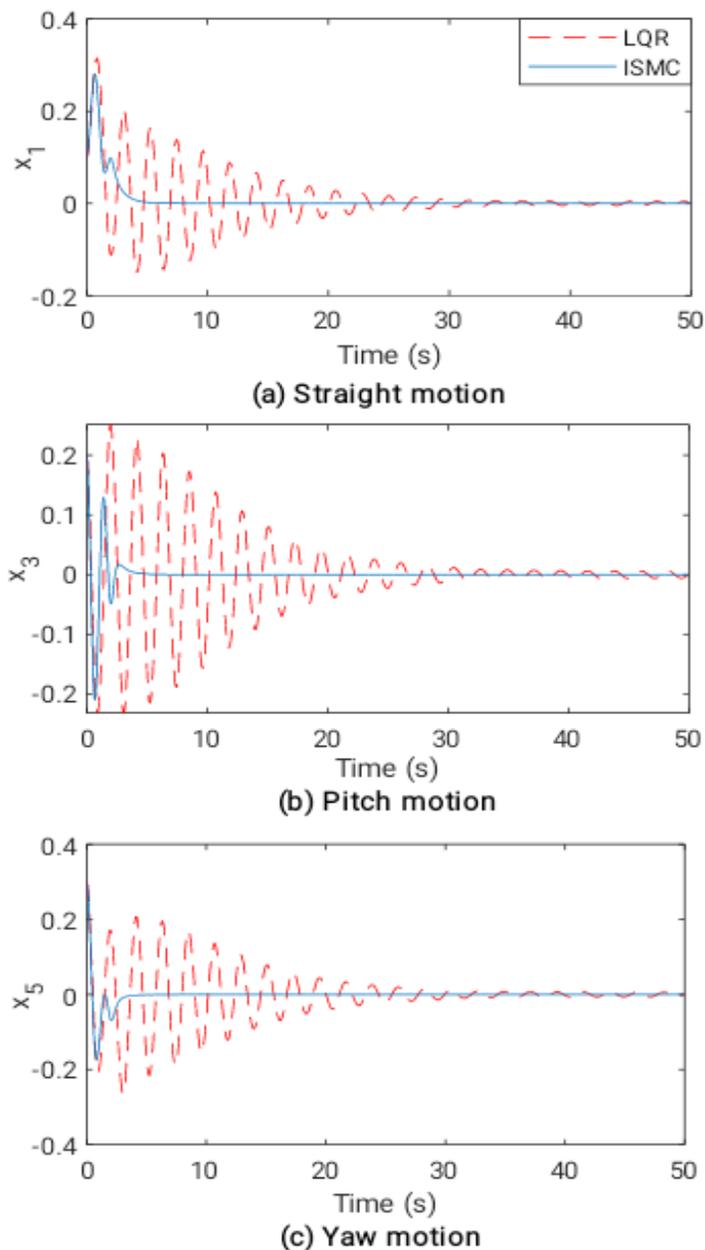
FIGURE 6

RESPONSE TO THE PARAMETER VARIATIONS

Error-values indicated in Table 2 depict the improvement in the performance of the proposed integral sliding mode controller over the linear quadratic regulator. From all the cases of the simulation, it can be seen that the performance of the proposed ISMC is superior to the LQR for constant and time-varying disturbances and parameter variations.

CONCLUSION

In this paper, a robust integral sliding mode control technique is proposed for the two-wheeled inverted pendulum. First, the modelling of the TWIP has been discussed with the MATLAB Simulink blocks. Then integral sliding mode controller is designed. MATLAB Simulink block diagrams for the system and controller are also presented. This scheme is then tested with continuous and constant disturbances.

TABLE 2.

COMPARISON OF ERROR PERFORMANCE INDICES.

Figure	Error Indices	Control	x_1	x_3	x_5
FIGURE 4	ITSE	ISMC	0.060	0.005	0.018
		LQR	0.225	0.017	0.700
	ITAE	ISMC	1.300	0.350	1.240
		LQR	13.00	3.400	27.00
FIGURE 5	ITSE	ISMC	0.060	0.005	0.018
		LQR	0.130	0.006	0.050
	ITAE	ISMC	0.900	0.150	0.280
		LQR	6.200	0.310	4.000
FIGURE 6	ITSE	ISMC	0.055	0.021	0.019
		LQR	0.640	1.100	1.100
	ITAE	ISMC	0.480	0.250	0.240
		LQR	10.00	13.00	14.00

Also, it is tested for parameter variations. The results are compared with LQR. From the simulation studies, it is found that the proposed ISMC provides satisfactory performance. The quantitative and qualitative comparison of the results is presented to show the efficacy of the recommended controller. The future work involves the hardware development of the system. This can be implemented with the full or reduced order estimator.

REFERENCES

[1] Castro, A., "Modeling and Dynamic Analysis of a Two-Wheeled Inverted Pendulum," MS Thesis, Georgia Institute of Technology, August 2012.

[2] Kim, S., and Kwon, S. J., "Dynamic Modeling of a Two-Wheeled Inverted Pendulum Balancing Mobile Robot," *International Journal of Control, Automation and Systems*, Vol. 13, No. 4, 2015, pp. 926-933.

[3] Xu, C., Li M., and Pan, F., "The system design and LQR control of a two-wheels self-balancing mobile robot," *International Conference on Electrical and Control Engineering*, 2011, pp. 2786-2789.

[4] Muhammad, M., Buyamin, S., Ahmad, M. N., Nawawi, S. W., and Ibrahim, Z., "Velocity Tracking Control of a Two-Wheeled Inverted Pendulum Robot: A Comparative Assessment between Partial Feedback Linearization and LQR Control Schemes," *International Review on Modelling and Simulations*, Vol. 5, 2012, pp. 1038-1048.

[5] Huang, C. H., Wang, W. J., and Chiu, C. H., "Design and Implementation of Fuzzy Control on a two-wheel Inverted Pendulum," *IEEE Transactions on Industrial Electronics*, Vol. 58, No. 7, July 2011, pp. 2988-3001.

[6] Muhammad, M., Buyamin, S., Ahmad, M. N., and Nawawi, S. W., "Takagi-Sugeno Fuzzy Modeling of a Two-wheeled Inverted Pendulum Robot," *Journal of Intelligent and Fuzzy Systems*, Vol. 25, 2013, pp. 535–546.

[7] Xu, J.-X., Guo, Z.-Q., and Lee, T. H., "Design and Implementation of Integral Sliding Mode Control on an Underactuated Two-Wheeled Mobile Robot," *IEEE Transactions on Industrial Electronics*, Vol. 61, No. 6, July 2014, pp. 3671-3681.

[8] Kim, S., and Kwon, S. J., "Nonlinear Optimal Control Design for Underactuated Two-Wheeled Inverted Pendulum Mobile Platform," *IEEE/ASME Transactions on Mechatronics*, Vol. 22, No. 6, December 2017, pp. 2803-2808.

[9] Murcia, H. F., and González, A. E., "Performance Comparison between PID and LQR Control on a 2-wheel Inverted Pendulum Robot," *Proceedings of IEEE Colombian Conference on Robotics and Automation*, Bogota, 2016, pp. 1-6.

[10] Prakash, K., and Thomas, K., "Study of Controllers for a Two-Wheeled Self-Balancing Robot," *Proceedings of International Conference on Next Generation Intelligent Systems*, Kottayam 2016, pp. 1-7.

[11] Zad, H. S., Ulasyar, A., Zohaib A., and Hussain, S. S., "Optimal Controller Design for Self-Balancing Two-Wheeled Robot System," *Proceedings of International Conference on Frontiers of Information Technology*, Islamabad, 2016, pp. 11-16.

[12] Shilpa, B., Indu, V., and Rajasree, S. R., "Design of an Underactuated Self-Balancing Robot using Linear Quadratic Regulator and Integral Sliding Mode Controller," *Proceedings of International Conference on Circuit, Power and Computing Technologies*, Kollam 2017, pp. 1-6.

[13] Wenxia, S., and Wei, C., "Simulation and Debugging of LQR Control for Two-Wheeled Self Balanced Robot," *Chinese Automation Congress*, Jinan, 2017, pp. 2391-2395.

[14] Pupek, L., and Dubay, R., "Velocity and Position Trajectory Tracking Through Sliding Mode Control of Two-Wheeled Self-balancing Mobile Robot," *Proceedings of Annual IEEE International Systems Conference*, Vancouver, BC, 2018, pp. 1-5.

[15] Al-Jlailaty, H., Jomaa, H., Daher, N., and Asmar, D., "Balancing a Two-Wheeled Mobile Robot using Adaptive Control," *Proceedings of IEEE International Multidisciplinary Conference on Engineering Technology*, Beirut, 2018, pp. 1-7.

[16] Imtiaz, M. A., Naveed, M., Bibi, N., Aziz, S., and Naqvi, S. Z. H., "Control System Design, Analysis & Implementation of Two-Wheeled Self Balancing Robot (TWSBR)," *Proceedings of IEEE 9th Annual Information Technology, Electronics and Mobile Communication Conference*, Vancouver, BC, 2018, pp. 431-437.

[17] Boucetta, Y., Ayad R., and Foitih, Z. A., "PID Controller with Robotic Arm using Optimization Algorithm," *International Journal of Mechanical Engineering*, Vol. 7, No. 2, 2022, pp. 3746–3751.

[18] Hasanah, N., Alasiry, A. H., and Sumantri, B., "Two Wheels Line Following Balancing Robot Control using Fuzzy Logic and PID on Sloping Surface," *International Electronics Symposium on Engineering Technology and Applications*, Bali, 2018, pp. 210-215.

[19] MATLAB: Simulink Control Design Toolbox User Manual, MathWorks, Version 4.5, 2017.

[20] Surjagade, P. V., Tiwari, A. P. and Shimjith, S. R., "Robust optimal integral sliding mode controller for total power control of large PHWRs," *IEEE Transactions on Nuclear Science*, Vol. 65, No. 7, 2018, pp. 1331–1344.

[21] Desai, R. J., Patre, B. M., Munje, R. K., Tiwari, A. P. and Shimjith, S. R., "Integral Sliding Mode for Power Distribution Control of Advanced Heavy Water Reactor," *IEEE Transactions on Nuclear Science*, Vol. 67, No. 6, June 2020, pp. 1076-1085.

[22] Gao, W., and Hung, J. C., "Variable structure control of nonlinear systems: a new approach," *IEEE Transactions on Industrial Electronics*, Vol. 40, No. 1, February 1993, pp. 45-55.